

pubs.acs.org/IECR Article

# Evidence for Size-Sieving Driven Vapor Sorption and Diffusion in a Glassy Polybenzoxazole Exhibiting Configurational Free Volume

William J. Box, Zihan Huang, Ruilan Guo, and Michele Galizia\*

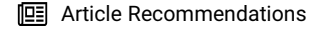


Cite This: Ind. Eng. Chem. Res. 2021, 60, 13326–13337



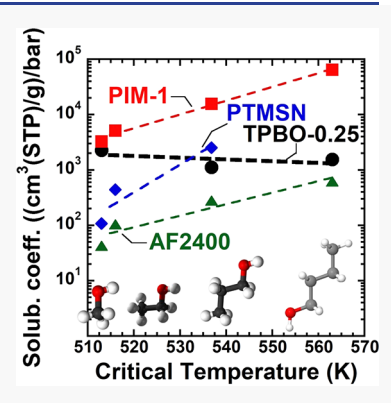
**ACCESS** 

III Metrics & More



Supporting Information

ABSTRACT: This paper reports, for the first time, the effect of configurational free volume (i.e., triptycene units) on condensable vapor transport in polymers. Alcohol and water vapor solubility and diffusivity isotherms at 25 °C in a triptycene-containing polybenzoxazole (TPBO) exhibiting configurational free volume are presented as a function of vapor activity, discussed, and used to develop fundamental structure—property correlations. This study provides evidence that while in conventional glassy polymers alcohol diffusion is size-controlled and sorption is enthalpy-controlled, which may create a trade-off between sorption-and diffusion-selectivity, alcohol sorption and diffusion in TPBO are both size-controlled, which makes it potentially easier to simultaneously tune sorption- and diffusion-selectivity to achieve highly selective separations. To put these results in a broad perspective, alcohol sorption and diffusion properties of TPBO were compared with those of conventional glassy polymers exhibiting conformational free volume, such as PIM-1, Teflon AF2400, polynorbornene, polysulfone, as well as rubbery PDMS. Finally, new exciting opportunities to exploit these unique TPBO's features for large scale molecular separations are discussed.



### 1. INTRODUCTION AND MOTIVATION

Membranes have become competitive among separation technologies. If we limit the discussion to gas separation, membranes currently cover about 20% of the market. The main advantage offered by membrane technology is the lower investment and operating costs relative to distillation and absorption, its compactness and modularity, as well as its energy efficiency. The latter represents a critical issue, considering that the US energy consumption for chemical separations is about 17,000 quadrillion Joule/year, which represents 50% of the total energy consumed by the American industry and 15% of the total energy consumed by the country in one year. The latter represents 50% of the total energy consumed by the country in one year.

Despite the available selection of membrane materials becoming increasingly diverse, as well as the membrane market continuing to see steady growth, the most popular membrane materials in the industry are relatively dated. Critical issues that hamper the membrane market to further expand are  $^{1,3-6}$  i) the permeability/selectivity trade-off, ii) the long-term instability of polymer transport properties due to physical aging, that is, the relaxation of excess conformational free volume over time, iii) the plasticization caused by highly sorbing species, which adversely affects membrane structure and long-term performance, and iv) difficulty in simultaneously maximizing sorptionand diffusion-selectivity, to achieve highly selective separations.

In recent years, a plethora of new materials appeared on the market, a few of which outperform the 2008 Robeson upper bound.<sup>7–9</sup> A special class of materials is defined by polymers exhibiting iptycene units (that is, triptycene and pentiptycene) in their backbone.<sup>7,10–15</sup> Iptycenes are 3D structures formed by three (cf. Figure 1) or five aromatic rings arranged in a

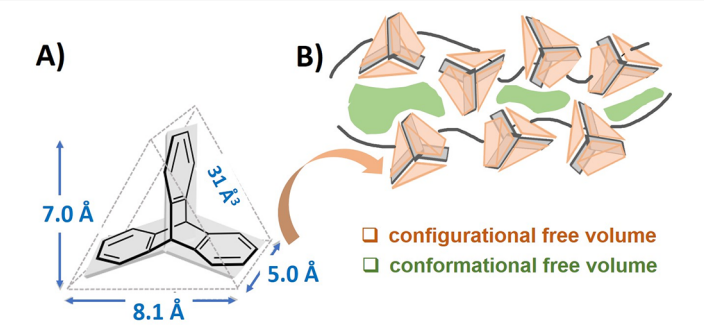


**Figure 1.** A) Structure and size of triptycene units. B) Conformational versus configurational free volume in glassy polymers.

paddlewheel-like configuration. The internal free volume of these structures is not related to the molecular conformation, such as the excess free volume in conventional glassy polymers, but to the molecular configuration.<sup>10</sup>

While conformational free volume originates from inefficient chain packing, which makes conventional glassy polymers susceptible to physical aging, 4,6 configurational free volume is intrinsic to the polymer structure, and as such, it is not

Received: July 6, 2021 Revised: August 18, 2021 Accepted: August 23, 2021 Published: September 1, 2021





collapsible. 10,16 Equally important, while the size of excess conformational free volume elements is randomly distributed, the internal volume of iptycene units is well-defined by the molecular configuration and is comparable to the size of a single molecule, which makes iptycene-based polymers highly selective in membrane separation applications. For example, benzotriptycene-based polymers of intrinsic microporosity reported by Comesaña-Gandara allowed a redefinition of the upper bound for several gas separations. It has been demonstrated that thermally rearranged polybenzoxazoles exhibiting configuration-based free volume (i.e., TPBOs), via the incorporation of iptycene units in the polyimide-precursor, abundantly surpass the 2008 upper bound and exhibit enhanced physical aging resistance compared to other new-generation polymers, even after a harsh thermal pretreatment.

Despite the *leitmotif* of configurational free volume appearing to be a promising strategy for the design of next generation polymer membranes, the fundamental mechanism of small molecule transport in iptycene-based polymers is not yet fully understood. In particular, the few published fundamental sorption and transport data in these materials refer to light gases, such as CH<sub>4</sub>, CO<sub>2</sub>, N<sub>2</sub>, and He, with little or no information available about the sorption and transport behavior of bulky condensable vapors. The scope of this study is to shed fundamental light on the influence of triptycene groups on vapor transport. Alcohols were chosen as model penetrants due to their importance as energy sources. Biofuels are, indeed, dilute alcohol/water mixtures, and energy-efficient separation technologies are crucially important to produce fuel-grade alcohols. <sup>18,19</sup>

While in conventional glassy polymers vapor diffusion is size-(i.e., entropy-) controlled and sorption is enthalpy-controlled, 1,20–22 which may create a trade-off between sorption-and diffusion-selectivity, this study provides evidence that vapor diffusion and sorption coefficients in TPBO are both size- (i.e., entropy-) controlled, which makes it easier to simultaneously tune sorption- and diffusion-selectivity to achieve highly selective molecular separations. This result comes from synergy between the exceptional size-sieving ability of iptycene units and the beneficial effect of size-controlled sorption. To the best of our knowledge, size-controlled sorption in polymers has never been reported before and will be the main object of investigation and discussion in this paper.

The unique transport mechanism of condensable vapors in TPBO as well as the lack of solubility in organic solvents make this material attractive for the separation of organic species via organic solvent nanofiltration (OSN) and reverse osmosis (OSRO), pervaporation as well as vapor permeation.<sup>23</sup> In this study, the vapor sorption and transport properties in TPBO are presented, thoroughly discussed, and used to develop fundamental structure—property correlations to serve as a guide to design iptycene-based materials for the separation of organic species in vapor and liquid phase.

# 2. THEORETICAL BACKGROUND

**2.1. Solution-Diffusion Model.** Small molecule transport in polymeric membranes that do not exhibit permanent pores is described in terms of the solution-diffusion model, based on which the permeability coefficient is given by the product of the sorption coefficient  $(S_i)$  and the concentration-averaged diffusion coefficient  $(\overline{D}_i)$ :<sup>24</sup>

$$P_i = \overline{D}_i \times S_i \tag{1}$$

The membrane ideal (that is, pure-component) selectivity,  $\alpha_{ij}$ , is given by the permeability ratio of the faster permeating species to that of the slower permeating species. Based on the solution-diffusion model, selectivity can be broken into a sorption (i.e., enthalpy-driven) contribution and a diffusion (i.e, entropy-driven) contribution: <sup>24</sup>

$$\alpha_{ij} = \frac{P_i}{P_j} = \frac{\bar{D}_i}{\bar{D}_j} \times \frac{S_i}{S_j} \tag{2}$$

Normally diffusion coefficient in polymers decreases with increasing penetrant molecular size, while the opposite behavior is observed for the sorption coefficient which, being controlled by penetrant condensability and mutual interactions, increases with increasing penetrant size. 1,24,25

**2.2. Equilibrium Sorption: GAB and Zimm–Lundberg Models.** The Guggenheim–Anderson–de Boer (GAB) model describes small molecule sorption in polymers as a function of penetrant activity.<sup>26–28</sup> The fundamental hypothesis underlying this model is that vapor molecules are adsorbed in multiple layers on the surface of a solid material. The model is parametrized as follows

$$C = \frac{C_p kAa}{(1 - ka)(1 - ka + Aka)} \tag{3}$$

where C is the amount of penetrant sorbed in the polymer, expressed in units of  $g/g_{pol}$  or  $cm^3(STP)/cm^3(polymer)$ , a is the penetrant activity (i.e., relative pressure defined as  $p/p_0$ , where p is the pressure, and  $p_0$  is the penetrant vapor pressure at the experimental temperature), and  $C_p$ , A, and k are the three model parameters. Specifically,  $C_p$  is the sorption capacity of the first monolayer of penetrant adsorbed on the polymer surface, A is the dimensionless heat of sorption of this first monolayer, and k describes the dimensionless heat of sorption of higher layers.

The Zimm-Lundberg clustering model<sup>29</sup> provides a pathway to predict penetrant clustering from the analysis of sorption isotherms. The Zimm-Lundberg clustering function is given by

$$\frac{G_{11}}{\tilde{V}_1} = (\phi_1 - 1) \left[ \frac{\partial {\binom{a/\phi_1}}}{\partial a} \right]_{T,p} - 1 \tag{4}$$

where  $G_{11}$  is the cluster integral,  $\tilde{V}_1$  is the partial molar volume of the penetrant,  $\phi_1$  is the penetrant volume fraction in the polymer

phase (i.e., 
$$\phi_1 = \frac{C\frac{\tilde{V}_1}{22414}}{\left(1 + C\frac{\tilde{V}_1}{22414}\right)}$$
, where  $C$  is the concentration

expressed in cm³(STP)/cm³(polymer),  $\tilde{V}_1$  is the penetrant molar volume in cm³/mol³0), and a is the penetrant activity. The size of the average cluster is given as  $\frac{\phi_1 G_{11}}{\tilde{V}_1} + 1$ . Clustering is considered to take place when the amount of molecules in a cluster is greater than 1, and the extent of clustering is given by the degree to which the cluster function is greater than -1. Fundamentally, this value quantifies the degree of nonrandom penetrant distribution within the polymer matrix.

**2.3.** Transient Sorption: Berens—Hopfenberg Models. In this study, transient diffusion is modeled using the Berens—Hopfenberg model, which generalizes the Fickian diffusion model by adding an exponential term that accounts for additional sorption due to polymer relaxation.<sup>31</sup> The Berens—Hopfenberg model is given as

Table 1. Structure and Properties of TPBO-0.25<sup>8</sup> and PIM-1<sup>36a</sup>

material	density	$T_g$	d-spacing
	(g/cm³)	(°C)	(Å)
<u>TPBO-0.25</u>			
CF <sub>3</sub> N N N N N N N N N N N N N N N N N N N	1.393 ±0.002	> 400	6.8
(CF3)			
<u>PIM-1</u>			
	1.143	442	6.6
"			

<sup>&</sup>lt;sup>a</sup>The latter is considered for comparison purposes.

$$M_{t} = M_{F} \left[ 1 - \frac{8}{\pi^{2}} \sum_{n=0}^{\infty} \frac{1}{(2n+1)^{2}} \exp(-(2n+1)^{2} k_{F} t) \right] + M_{r} [1 - \exp(-k_{r} t)]$$
(5)

where  $M_t$  is the total mass sorbed at time t,  $M_F$  and  $M_r$  refer to the mass contributions to equilibrium sorption due to Fickian diffusion and polymer relaxation, respectively, and  $k_F$  and  $k_r$  are the Fickian diffusion and polymer relaxation rate constants, expressed in units of inverse time. In low sorbing polymers, changes in vapor concentration at the polymer surface are negligible, therefore the Berens—Hopfenberg model can be used "as is". However, when considering highly sorbing vapors (such as methanol, in this study), the concentration at the polymer surface may change exponentially over time. <sup>32,33</sup> In this circumstance, a modified version of the Berens—Hopfenberg model must be used to estimate vapor diffusion coefficients from the analysis of experimental sorption kinetics, that is <sup>32</sup>

$$M_{t} = M_{F} \left[ 1 - \exp(-\beta t) \sqrt{\frac{4k_{F}}{\pi^{2}\beta}} \tan \sqrt{\frac{\pi^{2}\beta}{4k_{F}}} \right]$$

$$- \frac{8}{\pi^{2}} \sum_{n=0}^{\infty} \frac{\exp(-(2n+1)^{2}k_{F}t)}{(2n+1)^{2}[1 - (2n+1)^{2}k_{F}/\beta]} + M_{r}[1 - \exp(-k_{r}t)]$$
(6)

where  $\beta$  is a time constant, which is treated as an adjustable parameter. For all vapors studied except for methanol, the degree of sorption was small enough that the BH model (cf. eq 5) reasonably fits all transient sorption isotherms. In contrast, the modified Berens—Hopfenberg model (cf. eq 6) must be used to fit experimental methanol sorption kinetics in TPBO-0.25.

Once the Berens—Hopfenberg parameters are fit to transient sorption data, the vapor diffusion coefficient can be calculated as follows <sup>31,32</sup>

$$\bar{D}_i = \frac{k_F l^2}{\pi^2} \tag{7}$$

where l is the thickness of the polymer slab. Owing to the relatively low vapor sorption in TPBO-0.25, in eq 7, l corresponds to the thickness of the dry sample (i.e., prior to sorption experiment).

It is worth mentioning that eq 7 provides the concentrationaveraged diffusion coefficient, that is, the average diffusion coefficient within the concentration jump corresponding to each sorption step<sup>34</sup>

$$\bar{D}_{i} = \frac{1}{C_{i,2} - C_{i,1}} \int_{C_{i,1}}^{C_{i,2}} D_{i}^{eff}(C) dC$$
(8)

where  $D_i^{eff}$  is the effective, local diffusion coefficient (that is, the diffusion coefficient that would be estimated by applying an infinitesimal concentration jump), and  $C_{i,1}$  and  $C_{i,2}$  are the penetrant concentration in the polymer at the beginning and the end of any sorption step, respectively.

**2.4. Kinetic and Thermodynamic Contributions to the Diffusion Coefficient.** Small molecule diffusion coefficients in polymers can be decomposed into a purely kinetic term and a thermodynamic factor<sup>21</sup>

$$\bar{D}_i = \frac{L_i}{RT} \cdot \frac{\partial \mu_i}{\partial \ln (\omega_i)} = L_i \cdot \alpha_i \tag{9}$$

where  $L_i$  is the mobility coefficient or thermodynamically corrected diffusion coefficient, that is, the kinetic contribution to  $\overline{D}_i$ ,  $\alpha_i$  is the thermodynamic contribution, and  $\mu_i$  and  $\omega_i$  are the penetrant chemical potential and mass fraction in the polymer mixture, respectively. By applying the definition of activity in terms of chemical potential, the thermodynamic contribution can be expressed in terms of penetrant activity (that is,  $a_i$ ) as  $\alpha_i = \frac{\partial \ln{(a_i)}}{\partial \ln{(\omega_i)}}$ , allowing  $\alpha_i$  to be directly calculated from

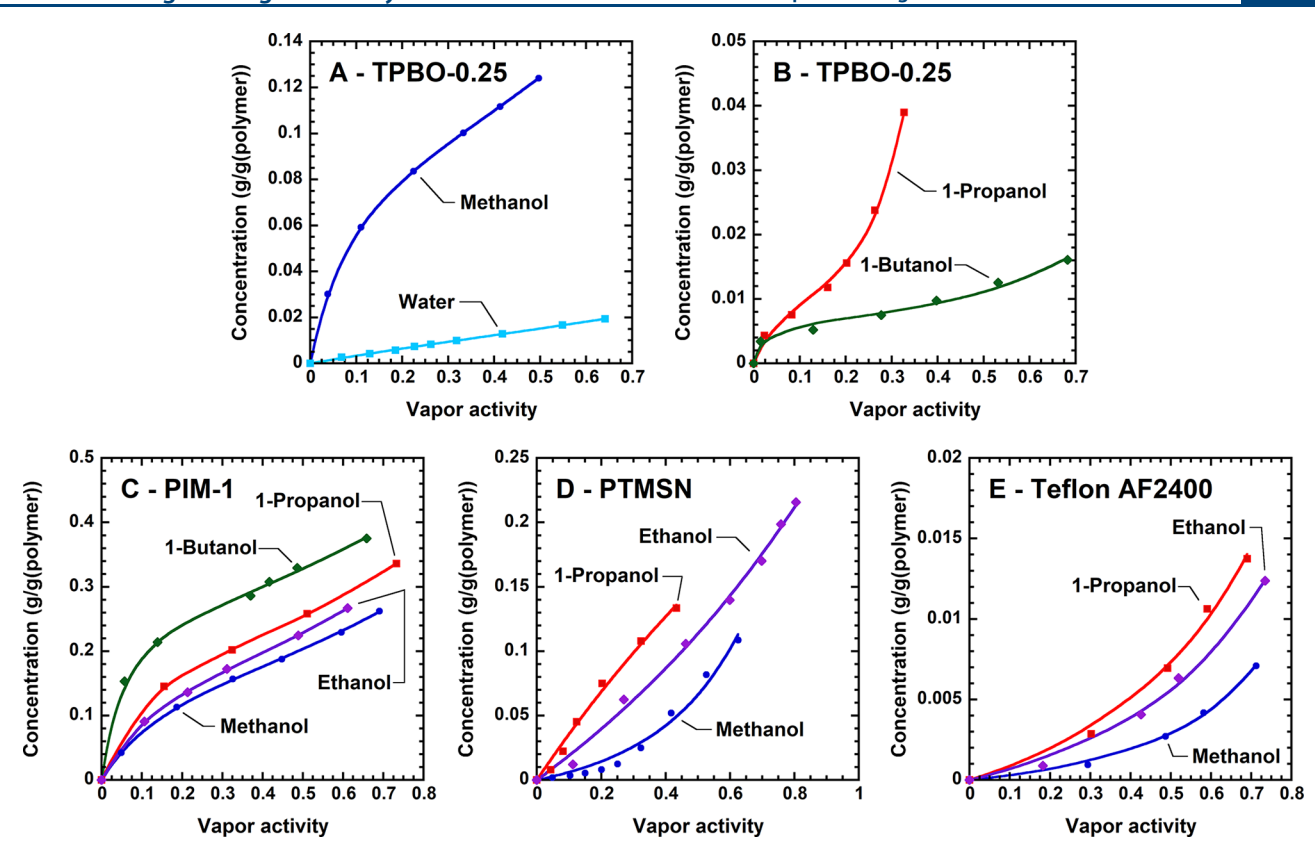


**Figure 2.** Experimental solubility isotherms: A) methanol and water at 25 °C in TPBO-0.25; B) 1-propanol and 1-butanol at 25 °C in TPBO-0.25; C) methanol, ethanol, 1-propanol, and 1-butanol in PIM-1 at 25 °C;  $^{36}$  D) methanol, ethanol, and 1-propanol in poly(trimethyl silyl norbornene) (PTMSN) at 35 °C;  $^{21}$  E) methanol, ethanol, and 1-propanol in Teflon AF2400 at 25 °C as a function of vapor activity.  $^{42}$  Solid lines are the GAB model fittings. Error bars for TPBO-0.25 sorption isotherms and activity values, which were calculated using linear error propagation, are too small to show.

equilibrium sorption isotherms. Finally, from  $\overline{D}_i$  and  $\alpha_i$ ,  $L_i$  can be obtained. As discussed in detail in previous studies,  $L_i$  represents a purely kinetic parameter which accounts for the frictional resistance offered by the polymer chains to penetrant diffusion;<sup>21</sup> it is related to penetrant molecular size as well as to the polymer structure. In contrast,  $\alpha_i$  measures the polymerpenetrant interactions. <sup>21</sup> If  $\alpha_i$  is larger than 1, polymer-penetrant interactions are favorable (i.e., attractive). In contrast, if  $\alpha_i$  is lower than 1, polymer-penetrant interactions are unfavorable (i.e., repulsive). Finally, if  $\alpha_i = 1$ , polymer-penetrant mixing is ideal, therefore  $\overline{D}_i = L_i$  (i.e., the diffusion coefficient does not need to be corrected for thermodynamic nonideality). This analysis of the diffusion coefficient is critically important when investigating vapor diffusion in polymers, due to the strong nonidealities occurring in these systems. 34,35 In contrast, light gases mix with polymers more ideally; therefore, correcting the diffusion coefficient for thermodynamic nonidealities is not strictly necessary.

### 3. EXPERIMENTAL METHODS

# **3.1.** Membrane Fabrication and Thermal Rearrangement. The material considered in this study is a thermally rearranged polybenzoxazole containing 25% mol of triptycene units, TPBO-0.25, fabricated from a copolyimide precursor with controlled triptycene molar content, i.e., triptycene-dianhydride(0.25)-6FDA(0.75)-6FAP(1.0). Details about the synthesis protocol of the triptycene-based poly(hydroxyimide) precursor are provided in previous studies and are summarized in the Supporting Information. Thermal rearrangement to polybenzoxazole was achieved by preheating the triptycene-

based poly(hydroxyimide) precursor at 300  $^{\circ}$ C under nitrogen purge for 2 h. Following this step, the temperature was raised to 450  $^{\circ}$ C at 10  $^{\circ}$ C/min and maintained for 30 min, after which the film was cooled down to room temperature (cooling rate = 10  $^{\circ}$ C/min), to get fully converted thermally rearranged samples (i.e., TPBO). The structure and physical properties of TPBO-0.25 are shown in Table 1, along with those of PIM-1, a standard microporous polymer that is considered for the sake of comparison throughout this paper.

3.2. Vapor Solubility and Diffusivity Measurements. Water and alcohol (i.e., methanol, 1-propanol, and 1-butanol) vapor sorption isotherms were collected at 25 °C using a constant-volume dual-chamber pressure decay system. The experimental setup consists of a precharge chamber, which houses the pressure transducer and where vapor is initially charged, and a sorption chamber, which houses the polymer sample. The experiment starts when the valve connecting the charge chamber to the sorption chamber is opened. Sorption is calculated from a molar balance, based on i) the pressure decay in the system, ii) the volume of the sorption and charge chambers, and iii) the temperature. Temperature was controlled using a Techne TU-20HT immersion circulator with an accuracy of ±0.005 °C, and pressure was measured using an MKS PDR2000 dual-capacitance manometer with a full scale of 500 Torr and an error of  $\pm 0.25\%$  of the reading. The charge and sorption chamber volumes were determined using the Burnett method<sup>37,38</sup> and found to be 29.477  $\pm$  0.098 cm<sup>3</sup> and 7.614  $\pm$ 0.023 cm<sup>3</sup>, respectively. Vapor was generated using a liquidphase penetrant stored in a vessel submerged in the water bath, connected to a valve upstream of the sampling and charge

chamber. Sorption measurements were conducted by initially pulling a vacuum in both the charge and sampling chambers and then allowing the vapor generator to fill the charge chamber to a certain pressure. The charge chamber pressure is measured, and the initial number of moles in the system is calculated using the ideal gas equation of state, due to the extremely low pressure in the system. Finally, the sampling chamber valve is opened, allowing vapor to reach the polymer, and equilibrium is reached once pressure decay ceases. A mole balance at equilibrium is then used to determine the number of moles sorbed into the polymer. Further sorption steps are repeated by charging additional vapor into the system.

Experimental sorption kinetics were fit to the Berens–Hopfenberg model to estimate the vapor diffusion coefficient,  $\bar{D}_{ij}$  as a function of concentration, as specified in the previous section. Before sorption begins, the polymer sample's thickness was measured using a Mitutoyo caliper with a resolution of 0.001 mm at multiple points and averaged. Experimental uncertainty of solubility and diffusivity data were calculated using linear error propagation. <sup>39,40</sup>

## 4. RESULTS AND DISCUSSION

**4.1. Equilibrium Vapor Sorption Isotherms.** Pure vapor sorption isotherms in TPBO-0.25 are shown in Figure 2A,B in units of g(penetrant)/g(pol) as a function of vapor activity. Equilibrium penetrant activity was calculated as  $a = p/p_0$ , where  $p_0$  was taken from NIST.<sup>41</sup>

Water and methanol sorption isotherms (cf., Figure 2A) follow the typical behavior observed in glassy polymers. Specifically, water vapor sorption isotherm is linear with activity, while methanol sorption isotherm exhibits the standard dual-mode behavior. <sup>43</sup> In sharp contrast, larger alcohols' (i.e., 1-propanol and 1-butanol, cf. Figure 2B) isotherms exhibit the dual-mode shape at activity below 0.1, with a prominent upturn at higher activities. The maximum uncertainty of sorption data, which was calculated using linear error propagation, was ±1.2%.

Figure 2A shows that methanol sorption in TPBO-0.25 is remarkably high, with a concentration exceeding 0.1 g/g(pol) starting from an activity of 0.35. This value is 40% lower than methanol solubility in PIM-1 at the same temperature<sup>36</sup> but much larger than the corresponding solubility in poly-(trimethylsilyl norbornene) (PTMSN)<sup>21</sup> and Teflon AF2400.<sup>42</sup>. PIM-1, PTMSN, and Teflon AF2400 were chosen as terms of comparison, as they also are high free volume glassy polymers exhibiting ultrahigh  $T_{\rm g}$  and for which vapor sorption data are available.

Interestingly, alcohol sorption in TPBO-0.25 markedly decreases with increasing condensability and molecular size (i.e., methanol ≫1-propanol >1-butanol, cf. Figure 2A,B). In sharp contrast, alcohol sorption in conventional glassy polymers, such as PIM-1, PTMSN, and Teflon AF, systematically increases with increasing condensability and molecular size (i.e., methanol < ethanol <1-propanol <1-butanol, cf. Figure 2C-E).  $^{21,36,42}$  It is well-known that small molecule sorption in polymers results from the interplay between enthalpic and entropic factors. 22,44,45 Enthalpic factors relate to polymer-penetrant interactions and penetrant condensability, according to the picture that penetrants exhibiting larger critical temperature (i.e., larger condensability) are more prone to sorb in the polymer phase in a condensed-like state. Entropic factors relate to penetrant molecular size, according to the physical picture that it becomes more difficult to accommodate penetrant molecules in the polymer matrix as their size increases (that is, sorption decreases

with decreasing configurational entropy). For most of the polymers studied in the literature, enthalpic effects overwhelm entropic effects; therefore, gas and vapor sorption systematically increase with increasing penetrant critical temperature (which means, in most cases, with increasing penetrant molecular size, cf. Table 2).<sup>20,21,36,45–47</sup> As shown in a previous study, this rule

Table 2. Critical Parameters and Kinetic Diameter of the Vapors Considered in This Study and in Vopicka's Study<sup>36</sup>

vapor	critical temperature 41 (K)	critical volume <sup>41</sup> (L/mol)	kinetic diameter <sup>49,50</sup> (Å)
water	647.0	0.0559	2.65
methanol	513.0	0.116	3.60
ethanol	516.2	0.168	4.50
1-propanol	536.9	0.217	4.70
1-butanol	563.1	0.274	5.00

applies to TPBO-0.25 when considering the sorption of light gases, so that gas solubility increases in the following order: CO<sub>2</sub>  $> CH_4 > N_2 > He.$  Interestingly, when considering bulky vapors sorption in TPBO-0.25, this rule is no longer valid. Even though a limited number of vapors have been investigated in this study, due to their slow sorption kinetics, TPBO-0.25 represents an interesting exception to the behavior described above, as alcohol sorption decreases with increasing condensability and molecular size. Alcohol polarity decreases with increasing the length of its organic tail; therefore, their interactions with hydrophobic polymers (such as PTMSN, PIM-1, and Teflon AF) become more thermodynamically favorable in the following order: methanol < ethanol < 1-propanol < 1-butanol. Therefore, enthalpic factors related to polymer-penetrant interactions and penetrant condensability make the sorption of bulkier alcohols in polymers larger than that of lower alcohols. <sup>21,36,42</sup> Analogous to PIM-1, PTMSN, and Teflon AF, TPBO-0.25 is a hydrophobic material, owing to its structure made of fused aromatic rings. Although the ether group on the TPBO-0.25 backbone exhibits some polarity, which would promote the sorption of lower polar alcohols, it is sterically shielded by the bulky triptycene unit in close proximity (cf. Table 1). This conclusion is supported by the fact that water vapor sorption in TPBO-0.25 and PIM-1 at 25 °C is fairly similar at low activity. At activity larger than 0.5, water sorption in TPBO-0.25 is even lower than is PIM-1 (cf. Figure S1, Supporting Information). Therefore, it does not seem reasonable to attribute the high sorption of lower alcohols in TPBO-0.25 to a favorable interaction between alcohol -OH groups and ether groups on the polymer backbone. We attribute this size-controlled sorption behavior in TPBO-0.25 to entropic factors. Indeed, while methanol (kinetic diameter = 3.6 Å, cf. Table 2) can fit in the internal cleft of triptycene units, bulkier alcohols are less likely to fit in the triptycene units, which could cause the observed size-exclusion effect. Different analyses, including PALS measurements and molecular simulations, provided an estimate of the size of the internal free volume of triptycene units. Specifically, PALS analysis conducted on TPBO-0.25 indicated that the average cavity size is about 7 Å.8 This number, however, does not provide the size of the internal free volume of triptycene units but the average size of free volume elements, including conformational and configurational free volume. A separate study indicated that the internal size of triptycene units is <4 Å.48 Finally, based on purely geometric considerations, one may consider the void space between two arene blades of triptycene units as a triangular

prism whose volume is 31 Å<sup>3</sup>. If this volume is approximated as that of a sphere, the diameter would be around 3.9 Å.<sup>48</sup> Therefore, we can infer that, among the alcohols considered in this study, only methanol can fit into the configurational free volume sites, while 1-propanol and 1-butanol are excluded, as their molecular size exceeds that of configurational free volume sites (cf. Table 2).

Sorption isotherms were fit to the GAB model (cf. eq 3 and Table 3). Uncertainty of the GAB parameters was calculated using the jackknife resampling method.<sup>51</sup>

Table 3. Fitted GAB Model Parameters for Vapor Sorption Isotherms in TPBO-0.25 at 25  $^{\circ}\text{C}$ 

vapor	$C_p\left(g/g(\text{pol})\right)$	A	k
water	$0.0233 \pm 0.00329$	$3.25 \pm 0.13$	$0.47 \pm 0.05$
methanol	$0.0962 \pm 0.0098$	$18.31 \pm 0.18$	$0.62 \pm 0.01$
1-propanol	$0.00914 \pm 0.00102$	$9.73 \pm 4.28$	$2.36 \pm 0.13$
1-butanol	$0.00601 \pm 0.00098$	$73.36 \pm 30.72$	$0.89 \pm 0.10$

As expected, the sorption capacity of the first alcohol monolayer,  $C_v$ , decreases with increasing the number of alcohol carbon atoms. This behavior, which is justified based on steric considerations, has been observed in other polymers, such as PIM-1.<sup>36</sup> The methanol  $C_p$  value, about 0.096 g/g(pol), is comparable to methanol total sorption, indicating that most of methanol is sorbed within the first monolayer, with negligible clustering. The same conclusion (i.e., lack of clustering) can be drawn for water, for which  $C_p$  is close to the total water concentration in the polymer. The parameter k measures the penetrant propensity to form clusters. While clustering looks negligible for water, methanol, and 1-butanol (for which k assumes relatively low values), 1-propanol is, among the vapors considered in this study, the one that clusters the most, based on its much larger k value. Finally, the heats of sorption of the first alcohol monolayer (A) do not follow a specific trend as a function of alcohol size, analogously to what was observed by Vopicka et al. in PIM-1.36

It should be noted that the relatively high uncertainty in parameter A is the result of the fact that the first monolayer usually becomes saturated within the first or second sorption step. This means that one or two data points contain the information needed to determine this parameter, and since parameter uncertainties in this work are determined using dropone-off (that is, jackknife) resampling, the loss of this data point produces a larger uncertainty on A.

The Zimm-Lundberg model was used to explain the prominent upturn in the sorption isotherms of higher alcohols and decouple the effects of swelling and clustering. The Zimm-Lundberg analysis shows clustering for 1-propanol, while methanol, water, and 1-butanol do not cluster according to this analysis (cf. Figure S2, Supporting Information). This picture is fully consistent with the results of the GAB fitting discussed above. However, we should note that the Zimm-Lundberg model provides a very empirical analysis of clustering; therefore, a FTIR-based investigation in underway to get a more realistic picture. Regardless, our analysis is still meaningful by way of the fact that two independent models (GAB and Zimm-Lundberg) point toward the same conclusions, as far as clustering is concerned. A still open question, however, is why methanol and water cluster less than 1-propanol. Due to its smaller alkyl tail, methanol is more polar than 1-propanol, and therefore, it is expected to exhibit a larger clustering propensity.

This result could be rationalized based on two effects: i) a fraction of sorbed methanol and water molecules (the only penetrants that can fit into the configurational free volume sites) are confined inside the triptycene units, which hampers methanol and water molecules to self-hydrogen bond; and ii) the polymer swelling produced by methanol, due to its extremely high sorption, creates additional room to accommodate the penetrant, which similarly hampers methanol molecules to get close enough to create higher order aggregates. The low methanol clustering propensity is consistent with the analysis of diffusion coefficients presented in section 4.2. Molecular simulations and experimental FTIR studies are underway to shed more light on this aspect. Finally, the higher 1-propanol clustering propensity relative to 1-butanol is consistent with the higher polarity of the former alcohol. The conclusion is that the upturn exhibited by the 1-butanol sorption isotherm is due to polymer swelling, while that exhibited by the 1-propanol sorption isotherm could be either due to polymer swelling or clustering. The analysis of diffusion coefficients will clarify this aspect (cf. section 4.2).

Koros et al. measured alcohol adsorption isotherms at 35 °C in zeolite imidazolate frameworks, namely ZIF-8, ZIF-71, and ZIF-90.<sup>52</sup> Although these isotherms exhibit a sigmoidal behavior at activity below 0.05, at activities above 0.1, sorption increases in the following order: methanol > ethanol  $\cong$  1-propanol. Krishna and co-workers combined experiments and Monte Carlo simulations to show that alkane sorption in zeolites is sizedriven (that is, entropy-driven), as it decreases with increasing the number of carbon atoms. They highlighted three types of entropic effects: a size effect, which favors the sorption of the component exhibiting the smallest number of carbon atoms, and a configurational effect, which, at given number of carbon atoms, favors the sorption of linear versus branched isomers. Finally, for zeolites exhibiting cylindrical channels, such as AFI and MOR, they highlighted a length effect, based on which sorption of double branched isomers is favored over linear alkanes. Therefore, an interesting similarity exists between vapor sorption in polymers exhibiting configurational free volume and sorbents.

Although it would be useful to include in this study other vapors besides alcohols, the time needed to reach sorption equilibrium in the presence of hydrocarbon vapors is unreasonably long. For this reason, in this preliminary study we limit our analysis to alcohol vapors.

**4.2. Vapor Diffusion Coefficient.** Vapor diffusion coefficients were determined as a function of vapor concentration in TPBO-0.25 from the analysis of the experimental sorption kinetics. As mentioned in the theoretical section, the Berens-Hopfenberg model was used to fit the experimental sorption kinetics of all vapors considered in this study, except for methanol. Due to its high solubility in TPBO-0.25, changes in methanol concentration at the polymer surface are expected; therefore, the modified Berens-Hopfenberg method was used in the latter case to provide a more accurate estimate of the diffusion coefficient. A comparison among different fitting approaches for methanol sorption kinetics is shown in Figure S3, Supporting Information. The models were implemented in *Julia* with an *n* cutoff of 15 (cf. eqs 5 and 6) and using LM-BFGS-B, a parameter optimization algorithm. As shown by Moon et al.,<sup>32</sup> considering more than 5 terms in eq 5 and 6 do not provide significant differences in the fitting quality. Examples of methanol and 1-propanol sorption kinetics in TPBO-0.25 at 25 °C, with the corresponding Berens-Hopfenberg fittings, are

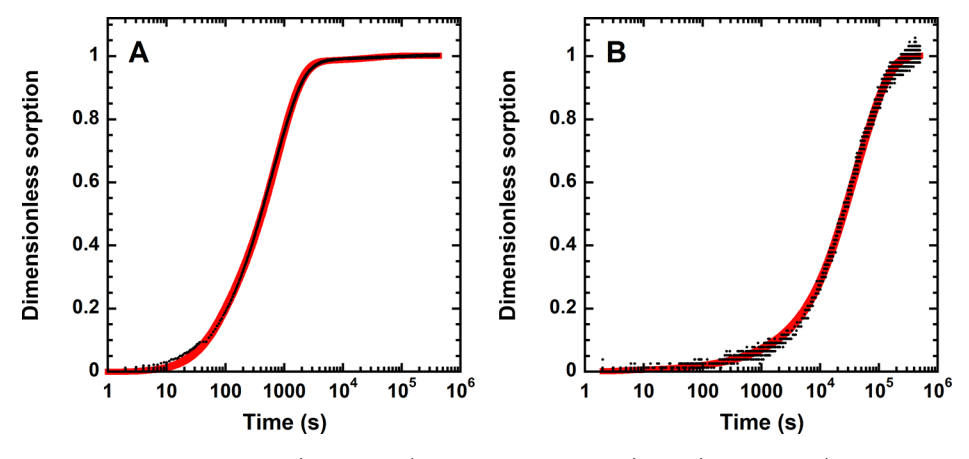


Figure 3. Sorption kinetics in TPBO-0.25 at 25 °C: A) methanol (activity jump 0.0–0.038) and B) 1-propanol (activity jump 0.16–0.20). Black dots are experimental data, and solid red lines are the modified Berens–Hopfenberg model (A) and the Berens–Hopfenberg model (B) fittings. 

31,32

Dimensionless sorption is defined as  $\frac{M_{sorbed}(t)}{M_{corbed}(t_{pc})}$ .

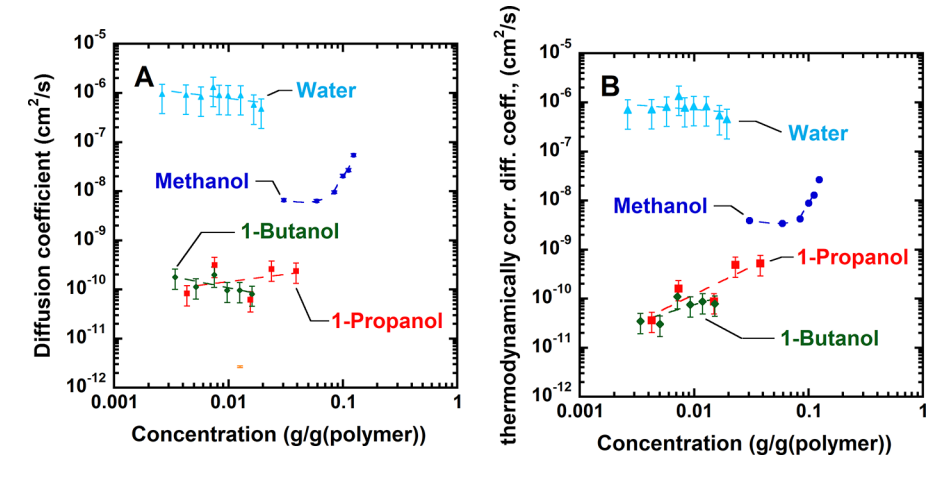


Figure 4. A) Vapor concentration-averaged diffusion coefficients,  $\overline{D}_{ij}$  in TPBO-0.25 at 25 °C as a function of equilibrium concentration. B) Mobility coefficients (i.e., thermodynamically corrected diffusion coefficients,  $L_i$ ) at 25 °C as a function of equilibrium concentration.

shown in Figure 3A,B. The best-fit parameters,  $k_E$ ,  $k_r$ , and  $\beta$ , are shown in Tables S1–S3, Supporting Information.

Vapor diffusion coefficients in TPBO-0.25 at 25 °C,  $\overline{D}_{\nu}$  are shown in Figure 4A as a function of vapor equilibrium concentration in the polymer. Experimental uncertainty of diffusion coefficients was calculated via bootstrap resampling.

As expected, diffusion coefficients decrease with increasing penetrant size in the following order: water > methanol >1-propanol ≅ 1-butanol. The trends of diffusion coefficients as a function of concentration, however, depend on the single vapor. For example, water and 1-propanol diffusion coefficients are fairly constant with concentration. In striking contrast, methanol diffusion coefficients increase markedly with increasing concentration. Finally, 1-butanol diffusion coefficients slightly decrease with increasing concentration in the polymer.

To properly analyze vapor diffusion in TPBO, it is recommendable to correct the diffusion coefficient for thermodynamic nonidealities. This correction is normally unnecessary for the analysis of light gas diffusion coefficients in polymers, due to the fact that the gas-polymer binary interactions do not depart substantially from ideal behavior, except in a limited number of cases. 47,54–57 However, this simplification does not necessarily apply to condensable vapors, whose mixing with the polymer to form a condensed-like phase may deviate considerably from ideality. 34,35 Vapor diffusion

coefficients in polymers are influenced by at least three factors:  $^{21,34,35}$  i) polymer relaxation and swelling, ii) vapor clustering, and iii) polymer—vapor molecular interactions. If we limit our analysis to the concentration-averaged diffusion coefficient,  $\bar{D}_i$  (cf., Figure 4A), these three effects are difficult to isolate; therefore, it is important to correct  $\bar{D}_i$  for thermodynamic nonidealities to get its purely kinetic component,  $L_i$  (i.e., the mobility factor, cf. Figure 4B).

Water mobility and diffusion coefficients are pretty constant with concentration, which is likely due to the low water concentration in the polymer. This fact, as well as the lack of water clustering shown by the GAB and Zimm-Lundberg models, indicates that water vapor does not plasticize TPBO-0.25. Therefore, we expect that humidity should not influence remarkably the TPBO performance in membrane applications.

As expected, mobility coefficients (cf. Figure 4B) systematically decrease with increasing penetrant size, which mirrors the behavior of the concentration-averaged diffusion coefficient. Interestingly, while 1-propanol and 1-butanol diffusion coefficients are very close to each other, the mobility coefficient of 1-propanol exceeds, as expected, that of 1-butanol. The methanol mobility coefficient is initially constant with increasing methanol concentration in the polymer, and then it increases. This result indicates that methanol molecules are initially accommodated in pre-existing sorption sites, which correspond to Langmuir sites

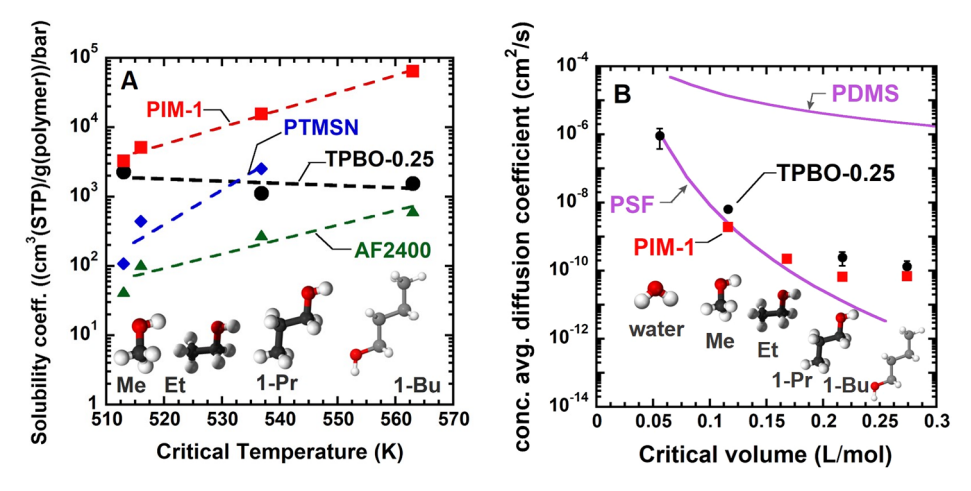


Figure 5. A) Vapor solubility coefficients, S, in (cm³(STP)/g(polymer))/bar, for various polymers as a function of vapor critical temperature. <sup>21,36,42</sup> TPBO-0.25 (black circles, 25 °C and activity 0.1). PIM-1 (red squares, 25 °C and activity 0.1). PTMSN (blue diamonds, 35 °C and activity 0.1). Teflon AF2400 (green triangles, 25 °C and activity 0.67). Dashed lines are drawn to guide the eye. B) Alcohol diffusion coefficients,  $\overline{D}_{ij}$  at 25 °C in PIM-1 (activity 0.2)<sup>36</sup> and TPBO-0.25 (activity 0.1) as a function of critical volume. Diffusivity data for poly(sulfone) (PSF) and PDMS at 25 °C are shown for the sake of comparison. <sup>59</sup>

in the traditional dual-mode nomenclature. 43 These sorption sites likely include triptycene units which, based on their size and geometry, may accommodate methanol molecules. At higher activities, polymer swelling pulls polymer chains apart and reduces the frictional resistance to penetrant transport, which may explain the increase in the methanol mobility coefficient. This picture is consistent with the results of the GAB and Zimm-Lundberg analyses, which rule out the occurrence of methanol clustering. The latter phenomenon, if present, would cause a decrease of methanol diffusivity with concentration, as clusters diffuse much more slowly compared to single molecules.<sup>30</sup> This conclusion, however, must be interpreted cautiously: as mentioned above, an FTIR investigation is underway to shed more light on the issue of clustering. We conclude that TPBO swelling caused by methanol sorption overwhelms methanol clustering. Ongoing molecular simulations will shed light on the possibility that a portion of methanol molecules is confined in the triptycene units, which would help rationalize the apparent lack of methanol clustering.

The 1-propanol and 1-butanol mobility coefficients increase with increasing penetrant concentration in the polymer, indicating that, also in this case, swelling overwhelms clustering.

**4.3. General Correlations and Comparison with Other Materials.** The equilibrium and transient sorption data discussed in sections 4.1 and 4.2 indicate that, while TPBO's vapor diffusion behavior does not depart from that of conventional polymers, its vapor sorption behavior is atypical. The penetrant sorption coefficient in polymers,  $S_{ij}$  is defined as follows  $^{22,47,58}$ 

$$S_i = C_i/p \tag{10}$$

where  $C_i$  is the equilibrium concentration, and p is the corresponding equilibrium pressure. It has been shown that the logarithm of the sorption coefficient increases linearly with increasing penetrant critical temperature<sup>45</sup> (i.e.,  $\ln(S_i) = \alpha + \beta T_C$ ).

In Figure 5A, the experimental alcohol sorption coefficients in PIM-1 at 25 °C and activity 0.1, reported by Vopicka et al., <sup>36</sup> systematically increase with increasing alcohol condensability and size. The same behavior has been observed in PTMSN at 35 °C<sup>21</sup> and Teflon AF2400 at 25 °C<sup>42</sup> (cf. Figure 5A). Even

though sorption data in TPBO-0.25 were collected for a limited number of vapors, due to the long times needed to reach equilibrium, the behavior of TPBO-0.25 deviates from that of conventional glassy polymers, as, at least for alcohols, sorption does not increase with increasing alcohol condensability and molecular size, but it exhibits a slightly decreasing trend (cf. Figure 5A). As discussed above, we hypothesize that, in contrast with conventional polymers, where alcohol sorption is enthalpy-driven, alcohol sorption in TPBO-0.25 is entropy-driven (i.e., size-driven). The unique size-driven sorption behavior exhibited by TPBO might originate from the extremely regular and rigid configuration-based free volume pockets provided by triptycene units, which are expected to control vapor sorption based on entropic factors instead of enthalpic factors.

The slope of the infinite dilution light gas solubility coefficient versus  $T_C$  (that is,  $\beta$ ) is about 0.016–0.020 K<sup>-1</sup> for hydrocarbonbased polymers and 0.009-0.012 K<sup>-1</sup> for perfluoropolymers.<sup>47</sup> The validity of this correlation for TPBO-0.25, PIM-1, and Teflon AF2400 has been verified in previous studies. 17,20,36,47 Specifically, when considering He, N<sub>2</sub>, CH<sub>4</sub>, and CO<sub>2</sub> sorption data at 35  $^{\circ}\mathrm{C}$  and in the limit of infinite dilution in TPBO-0.25,  $\beta$ = 0.015  $\mathrm{K}^{-1.^{17}}$  The kinetic diameter of He,  $\mathrm{N}_{\mathrm{2}}$ , CH<sub>4</sub>, and CO $_{\mathrm{2}}$  is smaller than the internal size of triptycene units, i.e., light gases can be accommodated into the configurational free volume delimited by the arene blades in the triptycene groups. As expected, the slope of the alcohol sorption coefficient versus  $T_C$ does not match the values shown above, due to profound differences between gas and vapor sorption. Indeed, in contrast with light gases, alcohol vapors i) give rise to mutual- and selfinteractions, ii) are much bulkier, and iii) produce a more severe polymer swelling, if not plasticization. Moreover, due to activity (i.e.,  $a = p/p_0$ ) limitations, vapor sorption isotherms contain less data points than light gas sorption isotherms; therefore, it is hard to provide a precise estimate of vapor sorption coefficients at infinite dilution. For this reason, the vapor sorption coefficients shown in Figure 5A are not taken at vanishing activity, which obviously complicates the comparison of  $\beta$  values among gases and vapors. A more detailed analysis of the  $\beta$  value for condensable vapor sorption in polymers would require solubility data for a variety of vapors exhibiting different properties (polarity, condensability, and size), while here we can rely only on 3 or 4 alcohols. For the sake of completeness, we report that, at 25 °C,  $\beta$  = 0.057 K<sup>-1</sup> for PIM-1 (considering methanol, ethanol, 1-propanol, and 1-butanol sorption data, cf. Figure 5A) and -0.0072 K<sup>-1</sup> for TPBO-0.25 (considering methanol, 1-propanol, and 1-butanol sorption data, cf. Figure 5A).

Vapor diffusion coefficients at 25 °C and activity 0.1 in TPBO-0.25 are shown in Figure 5B as a function of penetrant critical volume. Diffusivity data at 25 °C in PIM-1 (activity 0.2, ref 36) are shown as well for the sake of comparison. Alcohol diffusion coefficients in TPBO-0.25 slightly exceed those in PIM-1, which is consistent with the larger average *d*-spacing exhibited by TPBO-0.25 relative to PIM-1 (cf. Table 1). As expected, diffusion coefficients systematically decrease with increasing penetrant size; therefore, TPBO's behavior does not depart from that typically observed in other polymers.<sup>20</sup>

To put the results of this study in a broader perspective, diffusion coefficients in TPBO are compared to previously reported data for glassy polysulfone (PSF, a model size-selective polymer) and rubbery poly(dimethylsiloxane) (PDMS, a model soluble-selective polymer) at 25 °C. <sup>59</sup> As shown in Figure 5B, alcohol diffusion coefficients in TPBO lie close to those of glassy PSF, which demonstrates the TPBO size-sieving behavior.

The results discussed above indicate that both vapor sorption and diffusion coefficients in TPBO-0.25 are entropy-driven, that is, both vapor sorption and diffusion coefficients decrease with increasing vapor size. In conventional polymers, the vapor sorption coefficient increases with increasing penetrant size, and the diffusion coefficient decreases with increasing penetrant size, which may create a trade-off between sorption- and diffusion-selectivity. In contrast, vapor solubility-selectivity and diffusivity-selectivity in TPBO are both size-controlled (i.e., entropy-controlled) which, based on the solution-diffusion model, may help optimize selectivity in separations involving bulky organic species.

**4.4. Implications.** The unique entropy-based vapor sorption and transport mechanism exhibited by TPBO highlights an interesting synergy between solubility- and diffusivity-coefficients, both of which decrease with increasing penetrant size, allowing for solubility- and diffusivity-selectivities to work together, rather than against each other. This feature may help maximize selectivity in a variety of separations involving bulky organic species, such as organic solvent nanofiltration, organic solvent reverse osmosis, and vapor permeation. For example, these separations may beneficially impact the production of ethanol and biofuels. Ethanol is a common solvent in the pharmaceutical industry and can be contaminated with variable amounts of methanol and water at the end of the production process. Azeotropic and extractive distillation, which are used to efficiently separate ethanol from other alcohols and water, are energy intensive and require large investment costs; therefore, it could be convenient to replace them with a membrane process.60

To highlight the practical implications of entropy-driven alcohol transport in TPBO-0.25, we report, in Table 4, the pure component 1-butanol/methanol sorption- and diffusion-selectivity estimated using the data shown in Figure 5A,B. While, in PIM-1, sorption-selectivity offsets the benefit of diffusion-selectivity, in TPBO-0.25, sorption- and diffusion-selectivity are both favorable to methanol. We want to stress that the numbers reported in Table 4 do not necessarily reflect the actual TPBO performance, as they are pure-vapor selectivities.

Table 4. Comparison between 1-Butanol/Methanol Sorption- and Diffusion-Selectivity at 25  $^{\circ}$ C in TPBO-0.25 and PIM-1 $^{c}$ 

	1-butanol/methanol sorption- selectivity <sup>a</sup>	$1\hbox{-butanol/methanol diffusion-} \\ \text{selectivity}^b$
TPBO- 0.25	$1.40 \pm 0.01$	$48 \pm 20$
PIM-1	0.050	28

"Estimated at an activity of 0.1. <sup>b</sup>Estimated at an activity of 0.2. Uncertainties for TPBO-0.25 were estimated using linear error propagation. <sup>c</sup>Data for PIM-1 are from ref 36.

## 5. CONCLUSIONS

Alcohol and water vapor equilibrium and transient sorption in a glassy polybenzoxazole exhibiting configurational free volume (TPBO-0.25) was studied experimentally at 25 °C as a function of vapor activity and compared to vapor transport in conventional glassy polymers exhibiting conformational free volume. Methanol sorption in TPBO-0.25, which is concave to the activity axis, is 40% lower than in PIM-1 and 50 times larger than in Teflon AF2400 at 25 °C. Sorption isotherms of higher alcohols, such as 1-propanol and 1-butanol, exhibit a marked upturn at activity above 0.2, which, based on the GAB and Zimm—Lundberg analysis, was attributed to polymer swelling.

In striking contrast with conventional glassy polymers, alcohol sorption in TPBO is entropy controlled, as it does not increase with increasing alcohol molecular size and critical temperature, with methanol (critical temperature = 239.9 °C, kinetic diameter = 3.6 Å) being the most soluble and 1-butanol (critical temperature = 289.9 °C, kinetic diameter = 5 Å) being the least soluble alcohol among those considered in this study. The opposite behavior is observed in conventional glassy polymers exhibiting conformational free volume, where vapor sorption is enthalpy driven and increases with increasing molecular size and condensability. This unique feature of TPBO was attributed to the triptycene units, which may effectively exclude molecules larger than their internal configurational free volume via a purely entropy-driven mechanism.

Vapor diffusion in TPBO-0.25 is accompanied by non-Fickian relaxation. Experimental vapor sorption kinetics were fit to the Berens-Hopfenberg diffusion-relaxation model, to get the concentration-averaged diffusion coefficient as a function of vapor concentration in the polymer. Concentration-averaged diffusion coefficients were then corrected for thermodynamic nonideality. Vapor diffusion coefficients in TPBO-0.25 at 25 °C lie close to the polysulfone values when reported as a function of vapor critical volume, which highlights the strong size-sieving ability exhibited by TPBO. Similar to conventional glassy polymers, vapor diffusion coefficients decrease with increasing vapor's molecular size. Therefore, vapor sorption and diffusion coefficients in TPBO-0.25 are both size-controlled, which makes it easier to simultaneously tune sorption-and diffusionselectivity to achieve highly selective separations. These unique features make TPBO an interesting candidate for vapor separations and, possibly, organic liquids separation.

Molecular simulations and FTIR-based investigations are in progress to shed more fundamental light on the unique mechanism of organic vapor and liquid transport in TPBO.

### ASSOCIATED CONTENT

### Supporting Information

The Supporting Information is available free of charge at https://pubs.acs.org/doi/10.1021/acs.iecr.1c02660.

Synthesis details for TPBO-0.25 and its polyimide precursor, water vapor sorption isotherms in TPBO-0.25 and PIM-1 at 25  $^{\circ}$ C, clustering function plot for TPBO-0.25, and Berens—Hopfenberg parameters and fitting details (PDF)

## AUTHOR INFORMATION

## **Corresponding Author**

Michele Galizia — School of Chemical, Biological and Materials Engineering, University of Oklahoma, Norman 73019 Oklahoma, United States; orcid.org/0000-0001-5430-4964; Email: mgalizia@ou.edu

### **Authors**

William J. Box — School of Chemical, Biological and Materials Engineering, University of Oklahoma, Norman 73019 Oklahoma, United States

**Zihan Huang** — Department of Chemical and Biomolecular Engineering, University of Notre Dame, Notre Dame 46556 Indiana, United States

Ruilan Guo – Department of Chemical and Biomolecular Engineering, University of Notre Dame, Notre Dame 46556 Indiana, United States; orcid.org/0000-0002-3373-2588

Complete contact information is available at: https://pubs.acs.org/10.1021/acs.iecr.1c02660

### **Notes**

The authors declare no competing financial interest. **Biographies** 



Will Box is a Ph.D. student in the Chemical, Biological, and Materials Engineering Department at the University of Oklahoma. He joined Professor Galizia's Membrane Laboratory after completing his bachelor's education in chemical engineering with special distinction at the same university. His research focuses on the fundamental understanding of the role of configurational free volume on small molecule transport in polymers by combining experiments with thermodynamic and kinetic models. He is also interested in applying machine learning to membrane materials design.



Zihan Huang joined the Chemical and Biomolecular Engineering Department at Notre Dame in the fall of 2017 as a Ph.D. student, after completing her bachelor's degree in Chemical Engineering from the University of California, San Diego. She is also a Graduate Fellow of the NSF Engineering Research Center CISTAR. Under the guidance of Prof. R. Guo, her doctoral research has focused on the development of iptycene-based microporous polymeric membranes for gas separation.



Ruilan Guo is the Frank M. Freimann Collegiate Associate Professor of Engineering of the Department of Chemical and Biomolecular Engineering at the University of Notre Dame. She earned her B.E. and M.E. in Materials Science & Engineering at Beijing University of Chemical Technology and her Ph.D. in Materials Science & Engineering from Georgia Tech. She was a postdoctoral fellow working with Prof. James E. McGrath at Virginia Tech before joining Notre Dame. Dr. Guo's research focuses on developing functional polymer materials for a wide range of applications including membranes for gas separations, polyelectrolyte membranes for fuel cells, ion-containing polymers for desalination, and water treatment. Dr. Guo is a recipient of the DOE Early Career Research Award, ACS Petroleum Research Fund for Doctoral New Investigators, Inaugural Class of Influential Researchers by I&EC Research (2017), and MSDE 2020 Emerging Investigators. She is currently a Thrust Lead of CISTAR, a NSF Engineering Research Center, and serves on the Editorial Advisory Board of ACS Applied Energy Materials.



Michele Galizia joined the OU Chemical Engineering Faculty in 2017, after completing his postdoctoral training at the University of Texas at Austin under the guidance of Profs. Benny Freeman and Don Paul. The Galizia Research Group exploits fundamental principles of physical chemistry and thermodynamics to design, characterize, and model polymer membranes for organic solvent reverse osmosis/nanofiltration and gas separation exhibiting preassigned selectivity and stability. Prof. Galizia has received a number of awards, including the NSF CAREER Award (2021), the 2021 Class of Influential Researchers by I&EC Research, the ACS-PRF New Doctoral Investigator, and the OU Chemical Engineering Outstanding Professor Award, among others. In 2018, the journal Frontiers in Polymer Chemistry (Nature Publishing Group) highlighted him as a rising star in membrane science. He is an Associate Editor of the Journal of Polymer Engineering and a member of the Editorial Board of the Journal of Membrane Science.

# ACKNOWLEDGMENTS

The authors acknowledge financial support from the US National Science Foundation (NSF) under the grant CBET-1926868 (*Interfacial Engineering*). This invited contribution is part of the I&EC Research special issue for the 2021 Class of Influential Researchers.

## REFERENCES

- (1) Galizia, M.; Chi, W. S.; Smith, Z. P.; Merkel, T. C.; Baker, R. W.; Freeman, B. D. 50th anniversary perspective: polymers and mixed matrix membranes for gas and vapor separation: a review and prospective opportunities. *Macromolecules* **2017**, *50* (20), 7809–7843.
- (2) Sholl, D. S.; Lively, R. P. Seven chemical separations to change the world. *Nature* **2016**, 532 (7600), 435.
- (3) Robeson, L. M. The upper bound revisited. J. Membr. Sci. 2008, 320 (1-2), 390-400.
- (4) Merrick, M. M.; Sujanani, R.; Freeman, B. D. Glassy polymers: Historical findings, membrane applications, and unresolved questions regarding physical aging. *Polymer* **2020**, *211*, 123176.
- (5) Abdulhamid, M. A.; Genduso, G.; Wang, Y.; Ma, X.; Pinnau, I. Plasticization-resistant carboxyl-functionalized 6FDA-polyimide of intrinsic microporosity (PIM-PI) for membrane-based gas separation. *Ind. Eng. Chem. Res.* **2020**, 59 (12), 5247–5256.
- (6) Huang, Y.; Paul, D. R. Physical aging of thin glassy polymer films monitored by gas permeability. *Polymer* **2004**, *45* (25), 8377–8393.
- (7) Comesaña-Gándara, B.; Chen, J.; Bezzu, C. G.; Carta, M.; Rose, I.; Ferrari, M.-C.; Esposito, E.; Fuoco, A.; Jansen, J. C.; McKeown, N. B. Redefining the Robeson upper bounds for CO 2/CH 4 and CO 2/N 2 separations using a series of ultrapermeable benzotriptycene-based polymers of intrinsic microporosity. *Energy Environ. Sci.* **2019**, *12* (9), 2733–2740.
- (8) Luo, S.; Zhang, Q.; Zhu, L.; Lin, H.; Kazanowska, B. A.; Doherty, C. M.; Hill, A. J.; Gao, P.; Guo, R. Highly selective and permeable

- microporous polymer membranes for hydrogen purification and CO2 removal from natural gas. *Chem. Mater.* **2018**, *30* (15), 5322–5332.
- (9) Corrado, T.; Guo, R. Macromolecular design strategies toward tailoring free volume in glassy polymers for high performance gas separation membranes. *Molecular Systems Design & Engineering* **2020**, *S* (1), 22–48.
- (10) Weidman, J. R.; Guo, R. The use of iptycenes in rational macromolecular design for gas separation membrane applications. *Ind. Eng. Chem. Res.* **2017**, *56* (15), 4220–4236.
- (11) Cho, Y. J.; Park, H. B. High performance polyimide with high internal free volume elements. *Macromol. Rapid Commun.* **2011**, 32 (7), 579–586.
- (12) Wiegand, J. R.; Smith, Z. P.; Liu, Q.; Patterson, C. T.; Freeman, B. D.; Guo, R. Synthesis and characterization of triptycene-based polyimides with tunable high fractional free volume for gas separation membranes. *J. Mater. Chem. A* **2014**, *2* (33), 13309–13320.
- (13) Luo, S.; Zhang, Q.; Bear, T. K.; Curtis, T. E.; Roeder, R. K.; Doherty, C. M.; Hill, A. J.; Guo, R. Triptycene-containing poly (benzoxazole-co-imide) membranes with enhanced mechanical strength for high-performance gas separation. *J. Membr. Sci.* **2018**, *551*, 305–314.
- (14) Ghanem, B. S.; Swaidan, R.; Litwiller, E.; Pinnau, I. Ultramicroporous triptycene-based polyimide membranes for high-performance gas separation. *Adv. Mater.* **2014**, *26* (22), 3688–3692.
- (15) Swaidan, R.; Ghanem, B.; Al-Saeedi, M.; Litwiller, E.; Pinnau, I. Role of intrachain rigidity in the plasticization of intrinsically microporous triptycene-based polyimide membranes in mixed-gas CO2/CH4 separations. *Macromolecules* **2014**, *47* (21), 7453–7462.
- (16) Crist, R. D.; Huang, Z.; Guo, R.; Galizia, M. Effect of thermal treatment on the structure and gas transport properties of a triptycene-based polybenzoxazole exhibiting configurational free volume. *J. Membr. Sci.* **2020**, *597*, 117759.
- (17) Loianno, V.; Luo, S.; Zhang, Q.; Guo, R.; Galizia, M. Gas and water vapor sorption and diffusion in a triptycene-based polybenzox-azole: effect of temperature and pressure and predicting of mixed gas sorption. *J. Membr. Sci.* **2019**, *574*, 100–111.
- (18) Turner, J. A. A realizable renewable energy future. *Science* **1999**, 285 (5428), 687–689.
- (19) Kumar, R.; Ghosh, A. K.; Pal, P. Sustainable production of biofuels through membrane-integrated systems. *Sep. Purif. Rev.* **2020**, 49 (3), 207–228.
- (20) Merkel, T.; Bondar, V.; Nagai, K.; Freeman, B.; Yampolskii, Y. P. Gas sorption, diffusion, and permeation in poly (2, 2-bis (trifluoromethyl)-4, 5-difluoro-1, 3-dioxole-co-tetrafluoroethylene). *Macromolecules* **1999**, 32 (25), 8427–8440.
- (21) Galizia, M.; De Angelis, M. G.; Finkelshtein, E.; Yampolskii, Y. P.; Sarti, G. C. Sorption and transport of hydrocarbons and alcohols in addition-type poly (trimethyl silyl norbornene). I: Experimental data. *J. Membr. Sci.* **2011**, *385*, 141–153.
- (22) Galizia, M.; De Angelis, M. G.; Sarti, G. C. Sorption of hydrocarbons and alcohols in addition-type poly (trimethyl silyl norbornene) and other high free volume glassy polymers. II: NELF model predictions. *J. Membr. Sci.* **2012**, *405*, 201–211.
- (23) Hajilary, N.; Rezakazemi, M.; Shirazian, S. Biofuel types and membrane separation. *Environ. Chem. Lett.* **2019**, *17* (1), 1–18.
- (24) Wijmans, J. G.; Baker, R. W. The solution-diffusion model: a review. J. Membr. Sci. 1995, 107(1-2), 1-21.
- (25) Galizia, M.; Stevens, K. A.; Paul, D. R.; Freeman, B. D. Modeling gas permeability and diffusivity in HAB-6FDA polyimide and its thermally rearranged analogs. *J. Membr. Sci.* **2017**, *537*, 83–92.
- (26) Guggenheim, E. A. Applications of statistical mechanics; Oxford University Press: New York, 1966.
- (27) Anderson, R. B. Modifications of the Brunauer, Emmett and Teller equation 1. J. Am. Chem. Soc. 1946, 68 (4), 686-691.
- (28) Timmermann, E. O. A BET-like three sorption stage isotherm. *J. Chem. Soc., Faraday Trans. 1* **1989**, 85 (7), 1631–1645.
- (29) Zimm, B. H.; Lundberg, J. L. Sorption of vapors by high polymers. J. Phys. Chem. 1956, 60 (4), 425–428.

- (30) Singh, A.; Freeman, B.; Pinnau, I. Pure and mixed gas acetone/nitrogen permeation properties of polydimethylsiloxane [PDMS]. *J. Polym. Sci., Part B: Polym. Phys.* **1998**, *36* (2), 289–301.
- (31) Berens, A. R.; Hopfenberg, H. B. Diffusion and relaxation in glassy polymer powders: 2. Separation of diffusion and relaxation parameters. *Polymer* 1978, 19 (5), 489–496.
- (32) Moon, J. D.; Galizia, M.; Borjigin, H.; Liu, R.; Riffle, J. S.; Freeman, B. D.; Paul, D. R. Water vapor sorption, diffusion, and dilation in polybenzimidazoles. *Macromolecules* **2018**, *51* (18), 7197–7208.
- (33) Crank, J. The mathematics of diffusion; Oxford University Press: 1979.
- (34) Bye, K. P.; Loianno, V.; Pham, T. N.; Liu, R.; Riffle, J. S.; Galizia, M. Pure and mixed fluid sorption and transport in Celazole® polybenzimidazole: Effect of plasticization. *J. Membr. Sci.* **2019**, *580*, 235–247.
- (35) Jue, M. L.; McKay, C. S.; McCool, B. A.; Finn, M.; Lively, R. P. Effect of Nonsolvent Treatments on the Microstructure of PIM-1. *Macromolecules* **2015**, *48* (16), 5780–5790.
- (36) Vopička, O.; Friess, K.; Hynek, V.; Sysel, P.; Zgažar, M.; Šípek, M.; Pilnáček, K.; Lanč, M.; Jansen, J. C.; Mason, C. R. Equilibrium and transient sorption of vapours and gases in the polymer of intrinsic microporosity PIM-1. *J. Membr. Sci.* **2013**, 434, 148–160.
- (37) Burnett, E. Compressibility determinations without volume measurements. *J. Appl. Mech.* **1936**, *3*, A136–A140.
- (38) Lin, H.; Freeman, B. Permeation and diffusion; Springer: New York, 2006; pp 371-387.
- (39) Bevington, P. R.; Robinson, D. K. Data reduction and error analysis; McGraw Hill: New York, 2003.
- (40) Giordano, M. Uncertainty propagation with functionally correlated quantities. 2016, arXiv:1610.08716. arXiv preprint. https://arxiv.org/abs/1610.08716 (accessed 2021-08-30).
- (41) Technology, N.-A. I. o. S. a. https://www.nist.gov/ (accessed 2020-06-29).
- (42) Friess, K.; Jansen, J. C.; Poživil, J.; Hanta, V.; Hynek, V.; Vopička, O. e.; Zgažar, M.; Bernardo, P.; Izák, P.; Drioli, E. Anomalous phenomena occurring during permeation and sorption of C1–C6 alcohol vapors in Teflon AF 2400. *Ind. Eng. Chem. Res.* **2013**, *52* (31), 10406–10417.
- (43) Koros, W. J.; Chan, A.; Paul, D. Sorption and transport of various gases in polycarbonate. *J. Membr. Sci.* **1977**, *2*, 165–190.
- (44) Loianno, V.; Zhang, Q.; Luo, S.; Guo, R.; Galizia, M. Modeling gas and vapor sorption and swelling in triptycene-based polybenzox-azole: evidence for entropy-driven sorption behavior. *Macromolecules* **2019**, 52 (11), 4385–4395.
- (45) Galizia, M.; Stevens, K. A.; Smith, Z. P.; Paul, D. R.; Freeman, B. D. Nonequilibrium lattice fluid modeling of gas solubility in HAB-6FDA polyimide and its thermally rearranged analogues. *Macromolecules* **2016**, 49 (22), 8768–8779.
- (46) De Angelis, M.; Sarti, G.; Doghieri, F. NELF model prediction of the infinite dilution gas solubility in glassy polymers. *J. Membr. Sci.* **2007**, 289 (1–2), 106–122.
- (47) Smith, Z. P.; Tiwari, R. R.; Dose, M. E.; Gleason, K. L.; Murphy, T. M.; Sanders, D. F.; Gunawan, G.; Robeson, L. M.; Paul, D. R.; Freeman, B. D. Influence of diffusivity and sorption on helium and hydrogen separations in hydrocarbon, silicon, and fluorocarbon-based polymers. *Macromolecules* **2014**, *47* (9), 3170–3184.
- (48) Weidman, J. R.; Luo, S.; Doherty, C. M.; Hill, A. J.; Gao, P.; Guo, R. Analysis of governing factors controlling gas transport through fresh and aged triptycene-based polyimide films. *J. Membr. Sci.* **2017**, *522*, 12–22.
- (49) Van Leeuwen, M. Derivation of Stockmayer potential parameters for polar fluids. Fluid Phase Equilib. 1994, 99, 1–18.
- (50) Bowen, T. C.; Li, S.; Noble, R. D.; Falconer, J. L. Driving force for pervaporation through zeolite membranes. *J. Membr. Sci.* **2003**, 225 (1–2), 165–176.
- (51) Friedl, H.; Stampfer, E. Jackknife resampling. In Wiley StatsRef: Statistics Reference Online; 2014; DOI: 10.1002/9781118445112.stat07185.

- (52) Zhang, K.; Lively, R. P.; Dose, M. E.; Brown, A. J.; Zhang, C.; Chung, J.; Nair, S.; Koros, W. J.; Chance, R. R. Alcohol and water adsorption in zeolitic imidazolate frameworks. *Chem. Commun.* **2013**, 49 (31), 3245–3247.
- (53) Krishna, R.; Smit, B.; Calero, S. Entropy effects during sorption of alkanes in zeolites. *Chem. Soc. Rev.* **2002**, *31* (3), 185–194.
- (54) Merkel, T. C.; Pinnau, I.; Prabhakar, R.; Freeman, B. D. Gas and vapor transport properties of perfluoropolymers. In *Materials Science of Membranes for Gas and Vapor Separation*; 2006; Vol. 1, p 251,.
- (55) Prabhakar, R.; Freeman, B. Application of hydrocarbon—fluorocarbon interactions in membrane-based gas separations. *Desalination* **2002**, *144* (1–3), 79–83.
- (56) Li, Y.; Yavari, M.; Baldanza, A.; Di Maio, E.; Okamoto, Y.; Lin, H.; Galizia, M. Volumetric Properties and Sorption Behavior of Perfluoropolymers with Dioxolane Pendant Rings. *Ind. Eng. Chem. Res.* **2020**, *59* (12), 5276–5286.
- (57) Omidvar, M.; Nguyen, H.; Liu, J.; Lin, H. Sorption-enhanced membrane materials for gas separation: a road less traveled. *Curr. Opin. Chem. Eng.* **2018**, 20, 50–59.
- (58) Körösy, F. Two rules concerning solubility of gases and crude data on solubility of krypton. *Trans. Faraday Soc.* **1937**, 33, 416–425.
- (59) Matteucci, S.; Yampolskii, Y.; Freeman, B. D.; Pinnau, I. Transport of gases and vapors in glassy and rubbery polymers. *Materials science of membranes for gas and vapor separation* **2006**, *1*, 1–2.
- (60) Dong, Y.; Dai, C.; Lei, Z. Separation of the Methanol–Ethanol–Water Mixture Using Ionic Liquid. *Ind. Eng. Chem. Res.* **2018**, *57* (32), 11167–11177.

### NOTE ADDED AFTER ASAP PUBLICATION

Published ASAP on September 1, 2021; revised September 2, 2021 to correct production error in eq 5.